SAND2008-6595P

Technical Reference on Hydrogen Compatibility of Materials

High-Alloy Ferritic Steels:
Duplex Stainless Steels (code 1600)

Prepared by:

J.A. Zelinski, Defense Nuclear Facilities Safety Board, Washington DC
C. San Marchi, Sandia National Laboratories, Livermore CA

Editors
C. San Marchi
B.P. Somerday
Sandia National Laboratories

This report may be updated and revised periodically in response to the needs of the technical community; up-to-date versions can be requested from the editors at the address given below or downloaded at http://www.ca.sandia.gov/matlsTechRef/ . The content of this report will also be incorporated into a Sandia National Laboratory report (SAND2008-1163); the most recent version can be obtained from the link above. The success of this reference depends upon feedback from the technical community; please forward your comments, suggestions, criticisms and relevant public-domain data to the authors C. San Marchi (cwsanma@sandia.gov) and/or B.P. Somerday (bpsomer@sandia.gov) at:

Sandia National Laboratories
Technical Reference on Hydrogen Compatibility of Materials
MS-9404
7011 East Ave
Livermore CA 94550.

This document was prepared with financial support from the Safety, Codes and Standards program element of the Hydrogen, Fuel Cells and Infrastructure program, Office of Energy Efficiency and Renewable Energy. Sandia is a multiprogram laboratory operated by Sandia Corporation, a Lockheed Martin Company, for the United States Department of Energy under contract DE-AC04-94AL85000.

September 2008

Technical Reference on Hydrogen Compatibility of Materials

High-Alloy Ferritic Steels:

Duplex Stainless Steels (code 1600)

1. General

A duplex stainless steel is an alloy containing a two-phase microstructure of face-centered cubic austenite (γ) and body-centered cubic ferrite (α), where the phases each consist of at least 12 wt% Cr. Generally, duplex stainless steels have compositions in the range 18-26 wt% Cr, 4-7 wt% Ni, and in many cases 2-3 wt% Mo with some nitrogen. The so-called super duplex stainless steels have alloy contents at (or even slightly greater than) the high end of these ranges. Duplex stainless steels are typically used in applications that benefit from their high resistance to stress corrosion cracking, good weldability, and greater strength than other stainless steels [1].

Given this two-phase microstructure, duplex stainless steels provide a mixture of the properties of each phase so that they are tougher than the ferritic steels and stronger than the (annealed) austenitic steels by a factor of about two. This implies that their compatibility with hydrogen also reflects a combination of the phases. Ferrite is highly susceptible to hydrogen-assisted fracture and has high diffusivity and low solubility for hydrogen. Austenite is generally much less susceptible to hydrogen-assisted fracture, but has a very high solubility and very low diffusivity for hydrogen. Consequently, the resistance to hydrogen-assisted fracture increases with austenite content [2]. A further consequence of the difference in transport of hydrogen in these two primary phases is that a fully ferritic steel recovers much of its ductility in a few days when removed from a hydrogen environment, while the presence of 15% austenite results in much less recovery after removal from a hydrogen environment [2]. No detectable recovery of ductility is noted in 2205 (35% austenite) thermally precharged with hydrogen then subsequently stored at ambient temperature for 3 years [2].

In general, duplex stainless steels with internal hydrogen experience significant losses in ductility as measured by reduction of area in smooth tensile tests [2-6]. Susceptibility to hydrogen-assisted fracture appears to be greater for material that has been strain-hardened compared to annealed material [6]. Ductility losses when tested in low-pressure hydrogen gas are less severe, although quite significant considering the hydrogen fugacity at low pressure. Effects of gaseous hydrogen on fracture are also manifest in notched specimens [7, 8] and fatigue [9, 10].

1.1 Composition and microstructure

Table 1.1.1 lists the approximate compositional specification ranges for a number of duplex alloys. Table 1.1.2 provides the compositions of several heats of duplex stainless steel used to study hydrogen effects. Table 1.1.3 summarizes the nominal tensile properties and austenite content of materials from several studies on hydrogen effects.

1.2 Common designations

Duplex stainless steels are often designated with four digits: the first two digits represent the weight percent of chromium, and the second two digits represent the weight percent of nickel; thus 2205 nominally has 22% Cr and 5% Ni. However, a number of duplex stainless steels have registered trademarks and tradenames associated with them such as Uranus 50, Zeron 100, and Ferralium 255. The more common alloys and their tradenames are summarized in Table 1.1.1.

2. Permeability, Diffusivity and Solubility

Hydrogen gas permeation experiments on duplex alloys have not been found in the literature. Perng and Altstetter, however, have performed gas phase permeation experiments on highly cold-worked type 301 and type 304 stainless steels that resulted in microstructures with large fractions of α' martensite [11]; martensite and ferrite are expected to have relatively similar hydrogen transport properties since both phases are body-centered cubic (while austenite is face-centered cubic). Their results show the diffusivity of the 301 austenite-martensite composite increases with content of martensite and approaches the value measured for a ferritic stainless steel at high concentrations of martensite. The permeability of the 301 composite is also generally between the fully austenitic alloys (low permeability) and the ferritic stainless steel (high permeability), except at the highest martensite contents where the permeability in the composite is greater than the ferritic stainless steel. The hydrogen solubility is the quotient of the permeability and the diffusivity, thus the hydrogen solubility of the composite material is again between the low solubility exhibited in the ferritic stainless steel and the high solubility in the austenitic alloys.

Electrochemical and off-gassing techniques have been used to determine the diffusivity of hydrogen atoms in duplex stainless steels. Because of the two-phase structure and, generally, anisotropic microstructure, hydrogen transport in duplex steels can be a function of orientation. Hutchings et al. [12, 13] found that hydrogen diffusivity in duplex stainless steel (heat H91) was greater when the hydrogen flux was parallel to the elongated grain structure, however, this effect was relatively modest: about a factor of two. They also report that the diffusivity is not strongly affected by austenite content (γ) in the range 44% to 15%, but the diffusivity increases rapidly as the material becomes fully ferritic. The ratio of diffusivity of the duplex alloy with no austenite and with 44% austenite is about 400 [13]. This trend is consistent with the inverse rule of mixtures reported for diffusivity by Iacoviello et al. [14] of the form

$$\frac{1}{D_{eff}} = \frac{\left(1 - f_\gamma\right)}{D_\alpha} + \frac{f_\gamma}{D_\gamma} \tag{1}$$

This is a variant of the form proposed elsewhere [15], where f_γ is the volume fraction of austenite and D_{eff} is the effective diffusivity of the alloy and D_i is the diffusivity of the individual phases. Similar to orientation effects and the effects of austenite content, cold-work was found to have only a small effect on diffusivity of 2205 duplex stainless steel [16]. The diffusivity values reported in these and several other studies are given in Figure 2.1.

Degradation of tensile ductility due to precharging with hydrogen can be precluded if the materials are removed from the hydrogen environment and heated [3]. However, it may take an extraordinarily long time to recover properties without heating [2, 14]. Significant degradation in

tensile ductility was found to remain in thermally precharged 2205 (~35% austenite) after 55 days [3] and 3 years [2] at room temperature, but nearly full recovery of ductility was achieved by heating at 573 K for 4 hours [3]. As described above, the hydrogen diffusivity is relatively insensitive to phase distribution for expected ranges (γ content from 25 to 50% or greater), thus recovery of properties is not expected to be a strong function of the relative amounts of austenite and ferrite or their morphology.

The concentration of hydrogen in a 2205 duplex stainless steel with about 35% austenite content (heat Z91A) was found to be about 20 wppm after precharging in 22 MPa H_2 gas at 623 K for 48h [2, 5]. Thermal precharging at the same temperature but a slightly lower pressure (17 MPa) resulted in hydrogen content of 15 wppm [4]. These conditions are reported to be sufficient to reach uniform saturation in tensile bars with a gauge diameter of 3.2 mm [2, 4, 5].

3. Mechanical Properties: Effects of Gaseous Hydrogen

3.1 Tensile Properties

3.1.1 Smooth Tensile Properties

Room temperature testing of smooth tensile specimens with internal hydrogen (by thermal precharging in hydrogen gas) shows significant loss in ductility [2-5] as shown in Figure 3.1.1.1 as a function of strain rate. This plot shows the general trend that susceptibility to hydrogen-assisted fracture is enhanced at low strain rates due to more time for hydrogen redistribution to susceptible features in the microstructure. In addition, both annealed and strain-hardened 2507 show a significant degradation of tensile ductility: RA as low as 25% for the hydrogen-precharged material in the strain-hardened condition (Table 3.1.1.1) [6].

Smooth tensile specimens strained in hydrogen gas (external hydrogen) generally show (Figure 3.1.1.2) an increased susceptibility to hydrogen-assisted fracture as the hydrogen pressure is increased [3, 5]. Figure 3.1.1.3 compares the absolute RA for a single heat of 2205, showing that the ductility loss is a function of hydrogen pressure. The higher susceptibility to hydrogen-assisted fracture at low strain rate in these figures is attributed to the effect of deformation rate on both hydrogen transport and martensitic transformations [5]: more hydrogen can be transported in longer tests. The role of martensitic transformations on hydrogen-assisted fracture in austenitic steels has not been fully resolved, but it appears that martensitic transformations, while perhaps not necessary for degradation of stainless steels in hydrogen environments [17], certainly exacerbate hydrogen-assisted fracture when they form [18].

Although it is expected that orientation of the microstructure in duplex stainless steels could play an important role in hydrogen-assisted fracture, tensile testing of 2205 pipe with internal hydrogen shows little effect of orientation [4]. Tensile specimens tested in low-pressure external hydrogen, however, do show some effect of orientation [3-5]. Moreover, banded microstructures show larger variations with orientation than comparatively isotropic microstructures [4]. For testing in environmental hydrogen without significant prior hydrogen exposure, hydrogen must be transported from the surface of the specimen into the lattice. Since hydrogen diffusivity is much greater in ferrite compared to austenite, the morphology and orientation of the ferrite with respect to the cross section of the tensile specimen should play an important role on relatively short time scales, such as those associated with tensile tests. For example, ferrite bands that are oriented perpendicular to the tensile axis will be more effective at transporting hydrogen to the

center of a tensile specimen than ferrite bands that are aligned along the tensile axis. Moreover, orientation effects will probably become more important at lower ferrite content because ferrite will be less contiguous at lower volume fractions.

3.1.2 Notched Tensile Properties

Notched tensile foils of Ferralium 255 (heat P88) suffer a significant reduction in notch tensile strength and elongation to fracture when tested in 0.11 MPa hydrogen gas compared to testing in air at ambient temperature [7]. At temperature ≥ 373 K, there is no difference in properties measured in air and 0.11 MPa hydrogen gas [7].

3.2 Fracture mechanics

3.2.1 Fracture toughness

A significant reduction in the fracture toughness of thermally-precharged 2507 was reported for material in the strain-hardened condition (Table 3.2.1.1) [6]. Although a fracture toughness (K_{IC}) of 48 MPa $m^{1/2}$ in the thermally precharged condition is significantly lower than the material in the absence of thermal precharging, this value is consistent with threshold stress intensity factors measured for low-alloy steels [19] that are used in high-pressure hydrogen service.

3.2.2 Threshold stress-intensity factor

Altstetter et al. determined crack growth rates and threshold stress-intensity factors in notched sheet specimens of Ferralium 255 (heat P88) where plane stress conditions prevailed [7, 20]. Specimens were tested in up to 0.22 MPa hydrogen gas [7] and precharged to uniform concentration in molten salts at temperature of 538 K (i.e., internal hydrogen) [20]. These studies found that threshold values decreased as hydrogen pressure increased. The threshold values were also greater at elevated temperature for tests performed in hydrogen gas, particularly for tests at 348 K and 373 K [7].

Classic microvoid coalescence was observed on the fracture surfaces of precharged specimens at low hydrogen contents, while the amount of flat cleavage facets was greater for specimens with greater hydrogen content [20]. Threshold stress-intensity factors with internal hydrogen were relatively unaffected by testing temperature in the range 273 and 323 K [20].

3.3 Fatigue

Fatigue testing of a 2507 super duplex stainless steel (M92) in flowing hydrogen gas (i.e. hydrogen at approximately one atmosphere pressure) resulted in crack growth rates that are almost an order of magnitude higher than in argon for $\Delta K > 25$ MPa $m^{1/2}$ with R = 0.5 (ratio of minimum to maximum K and load) [10]. The crack growth rates, however, were similar for small stress intensity range (ΔK), less than about 15 MPa $m^{1/2}$ [10]. The upper and lower bounds of crack growth rates as a function of ΔK from Ref. [10] are shown in Figure 3.3.1. Crack growth rates also tended to be faster for greater R ratios although they become similar at $\Delta K >$ 30 MPa $m^{1/2}$ [10]. Fractography in this study showed that the ferrite failed by cleavage. A subsequent study [9] found that temperature in the range 298 K to 453 K had little effect on fatigue crack growth rates in flowing hydrogen.

3.4 Creep

No known published data in hydrogen gas.

3.5 Impact

No known published data in hydrogen gas.

3.6 Disk rupture testing

Disk rupture tests have been performed on duplex alloys referred to as 326 [21] and IN744 [22]; these alloys appear to be similar to one another with nominally 26Cr-7Ni and no molybdenum. Duplex stainless steel is classified as displaying little or no sensitivity to hydrogen in these studies and particularly attractive due to its high-strength [21]. This is at odds with the tensile and fracture mechanics data outlined in previous sections, perhaps due to the relative short-time scales associated with the disk rupture tests precluding substantial hydrogen transport in the lattice.

4. Fabrication

4.1 Primary processing

The resistance to hydrogen-assisted fracture of a 2205 duplex stainless steel (heat E96) was found to increase with austenite content in tensile testing in external hydrogen (0.2 MPa hydrogen gas) and with internal hydrogen (thermal precharging in 25 MPa hydrogen gas at 633 K) [2]. The observation that austenitic phases in duplex steels are more resistant to hydrogen-assisted fracture than ferritic phases is consistent with the view that austenitic stainless steels are relatively resistant to hydrogen-assisted fracture compared to ferritic steels [23].

4.2 Heat Treatment

Heat treatment was used to produce between about 5 and 50% austenite in duplex stainless steel 2205. The RA (both with internal and external hydrogen) was found to drop from greater than 50% to less than 20% as the amount of austenite was reduced (Figure 4.1.1) [2]. The trend for strain rate effects was similar for all microstructures (see Section 3.1.1). The effect of austenite content, however, must be balanced with the fact that the yield strengths of the microstructures with high austenite contents were somewhat lower (600 MPa compared to 750 MPa) than the microstructures with low austenite content (Table 1.1.3); hydrogen effects tend to be more pronounced in higher strength alloys.

4.3 Properties of welds

Laser welded notched tensile specimens from 2205 plate (heat Y05) were tested in 0.2 MPa gaseous hydrogen and reported in Ref. [8]. The austenite content in the weld was varied by controlling the welding process and it was found that material with higher austenite content showed greater resistance to hydrogen. The notched tensile strength (σ_s) of the base material (43% austenitic) was reduced by 9% when testing in hydrogen gas, while the σ_s of a weld with only 25% austenite was reduced by 28% in hydrogen gas.

Susceptibility to hydrogen-assisted fracture of duplex stainless steel increases markedly when the delta ferrite content is increased above 50% in weld deposits produced using an Ar-10 vol%

H_2 shielding gas [24]. Hydrogen-bearing shielding gases are used to improve weld pool fluidity and prevent surface oxidation, but hydrogen is entrapped in the microstructure during the welding process, increasing hydrogen susceptibility.

5. References

1. RA Lula. Stainless Steel (revised from "An Introduction to Stainless Steel" by JG Parr and A Hanson). Metals Park OH: American Society for Metals (1986).
2. AA El-Yazgi and D Hardie. Effect of heat treatment on susceptibility of duplex stainless steel to embrittlement by hydrogen. Mater Sci Technol 16 (2000) 506-510.
3. W Zheng and D Hardie. The effect of hydrogen on the fracture of a commercial duplex stainless steel. Corros Sci 32 (1991) 23-36.
4. W Zheng and D Hardie. Effect of structural orientation on the susceptibility of commercial duplex stainless steel to hydrogen embrittelement. Corrosion 47 (1991) 792-799.
5. AA El-Yazgi and D Hardie. The embrittlement of a duplex stainless steel by hydrogen in a variety of environments. Corros Sci 38 (1996) 735-744.
6. C San Marchi, BP Somerday, J Zelinski, X Tang and GH Schiroky. Mechanical properties of super duplex stainless steel 2507 after gas phase thermal precharging with hydrogen. Metall Mater Trans 38A (2007) 2763-2775.
7. T-P Perng and CJ Altstetter. Cracking Kinetics of Two-Phase Stainless Steel Alloys in Hydrogen Gas. Metall Trans 19A (1988) 145-152.
8. MC Young, SLI Chan, LW Tsay and CS Shin. Hydrogen-enhanced cracking of 2205 duplex stainless steel welds. Mater Chem Phys 91 (2005) 21-27.
9. TJ Marrow, PJ Cotterill and JE King. Temperature effects on the mechanism of time independent hydrogen assisted fatigue crack propagation in steels. Acta Metall Mater 40 (1992) 2059-2068.
10. TJ Marrow, CA Hippsley and JE King. Effect of mean stress on hydrogen assisted fatigue crack propagation in duplex stainless steel. Acta Metall Mater 39 (1991) 1367-1376.
11. T-P Perng and CJ Altstetter. Effects of Deformation on Hydrogen Permeation in Austenitic Stainless Steels. Acta Metall 34 (1986) 1771-1781.
12. RB Hutchings, A Turnbull and AT May. Measurement of hydrogen transport in a duplex stainless steel. Scr Metall Mater 25 (1991) 2657-2662.
13. A Turnbull and RB Hutchings. Analysis of hydrogen atom transport in a two-phase alloy. Mater Sci Eng A177 (1994) 161-171.
14. F Iacoviello, M Habashi and M Cavallini. Hydrogen embrittlement in the duplex stainless steel Z2CND2205 hydrogen-charged at 200˚C. Mater Sci Eng A224 (1997) 116-124.
15. U Bernabai and R Torella. Thermal analysis of hydrogen-charged austenitic and duplex stainless steel. Int J Hydrogen Energy 18 (1993) 763-771.
16. SS Chen, TI Wu and JK Wu. Effects of deformation on hydrogen degradation in a duplex stainless steel. J Mater Sci 39 (2004) 67-71.
17. AW Thompson. Ductility Losses in Austenitic Stainless Steels Caused by Hydrogen. in: IM Bernstein and AW Thompson, editors. Proceedings of the International Conference on the Effects of Hydrogen on Materials Properties and Selection and Structural Design: Hydrogen in Metals, 1973, Champion PA. American Society of Metals (1974) p. 91-105.
18. G Han, J He, S Fukuyama and K Yokogawa. Effect of strain-induced martensite on hydrogen environment embrittlement of sensitized austenitic stainless steels at low temperatures. Acta Mater 46 (1998) 4559-4570.

19. AW Loginow and EH Phelps. Steels for Seamless Hydrogen Pressure Vessels. Corrosion 31 (1975) 404-12.
20. J-H Huang and CJ Altstetter. Cracking of Duplex Stainless Steel Due to Dissolved Hydrogen. Metall Mater Trans 26A (1995) 1079-1085.
21. PF Azou and JP Fidelle. Very low strain rate hydrogen gas embrittlement (HGE) and fractography of high-strength, mainly austenitic stainless steels. in: MR Louthan, RP McNitt and RD Sisson, editors. Environmental Degradation of Engineering Materials III, 1987, The Pennsylvania State University, University Park PA. The Pennsylvania State University, University Park PA p. 189-198.
22. J-P Fidelle, R Bernardi, R Broudeur, C Roux and M Rapin. Disk Pressure Testing of Hydrogen Environment Embrittlement. in: Hydrogen Embrittlement Testing, ASTM STP 543, American Society for Testing and Materials. (1974) p. 221-253.
23. RJ Walter and WT Chandler. Influence of Gaseous Hydrogen on Metals: Final Report. Rocketdyne for the National Aeronautics and Space Administration, Canoga Park CA (Oct 1973).
24. K Shinozaki, L Ke and TH North. Hydrogen cracking in duplex stainless steel weld metal. Welding Journal 71 (1992) S387-S396.
25. ASTM. ASTM DS-56H, Metals and Alloys in the UNIFIED NUMBERING SYSTEM (SAE HS-1086 OCT01). 2001.
26. SL Chou and WT Tsai. Effect of grain size on the hydrogen-assisted cracking in duplex stainless steels. Mater Sci Eng A270 (1999) 219-224.
27. WC Luu, PK Liu and JK Wu. Hydrogen transport and degradation of a commercial duplex stainless steel. Corros Sci 44 (2002) 1783-1791.

Table 1.1.1. Compositions (wt%) of several common commercial duplex stainless steels [25].

UNS No	AISI No / Common Name	Fe	Cr	Ni	Mo	Cu	Mn	Si	C	N	other
S32101	LDX 2101	Bal	21.0 22.0	1.35 1.7	0.1 0.8	0.1 0.8	4.0 6.0	1.0 max	0.04 max	0.20 0.25	0.04 max P; 0.3 max S
S32205	2205	Bal	22.0 23.0	4.5 6.5	3.0 3.5	—	2.0 max	1.0 max	0.03 max	0.14 0.20	0.03 max P; 0.02 max S
S32304	2304	Bal	21.5 24.5	3.0 5.5	0.05 0.60	0.05 0.6	2.5 max	1.0 max	0.03 max	0.05 0.20	0.04 max P; 0.04 max S
S32404	Uranus 50 (Uranus B50)	Bal	20.5 22.5	5.5 8.5	2.0 3.0	1.0 2.0	2.0 max	1.0 max	0.04 max	0.2 max	0.03 max P; 0.01 max S
S32520	Uranus 52N+	Bal	24.0 26.0	5.5 8.0	3.0 4.0	0.5 2.0	1.5 max	0.8 max	0.03 max	0.20 0.35	0.035 max P; 0.02 max S
S32550	Ferralium 255	Bal	24.0 27.0	4.5 6.5	2.9 3.9	1.5 2.5	1.5 max	1.0 max	0.04 max	0.10 0.25	0.04 max P; 0.03 max S
S32750	SAF 2507	Bal	24.0 26.0	6.0 8.0	3.0 5.0	—	1.2 max	0.8 max	0.03 max	0.24 0.32	0.035 max P; 0.02 max S
S32760	Zeron 100	Bal	24.0 26.0	6.0 8.0	3.0 4.0	0.5 1.0	1.0 max	1.0 max	0.03 max	0.2 0.3	0.5-1.0 W; 0.03 max P; 0.01 max S
S32900	329	Bal	23.0 28.0	2.5 5.0	1.0 2.0	—	1.0 max	0.75 max	0.08 max	—	0.04 max P; 0.03 max S

Table 1.1.2. Compositions (wt%) of several heats of duplex stainless steels used to study hydrogen effects.

Heat	Alloy	Fe	Cr	Ni	Mo	Cu	Mn	Si	C	N	Other	Ref.
P88	Ferralium 255	Bal	26	5.5	3	1.6	nr	nr	nr	0.16	nr	[7]
H91	Uranus 50	Bal	21.6	6.3	2.51	0.77	0.63	0.87	0.06	nr	<0.01 P; 0.01 S	[12, 13]
M91	Zeron 100	Bal	24.04	6.827	3.77	0.626	0.77	0.175	0.024	0.215	0.025 P; 0.002 S; 0.625 W	[9, 10]
Z91A	2205	Bal	22.3	5.7	2.9	0.06	1.62	0.35	0.027	nr	0.021 P; <0.002 S	[4]
Z91B		Bal	22.9	5.2	3.12	0.03	0.99	0.5	0.016	nr	0.019 P; 0.002S	[3, 4]
E96	2205	Bal	23.0	5.0	3.0	nr	1.0	nr	nr	0.13	nr	[2, 5]
I97	Similar to 2205	Bal	22.78	5.64	2.5	0.15	1.43	0.39	0.03	0.13	0.028 P; 0.011 S	[14]
C99A	2205	Bal	22.15	5.28	3.11	—	1.58	0.53	0.024	0.19	0.028 P; 0.002 S	[26]
C99B		Bal	22.4	5.42	3.24	0.21	1.43	0.41	0.014	0.198	0.025 P; 0.004 S	
L02	2205	Bal	22.79	5.32	3	0.04	1.53	0.37	0.03	0.2	0.03 P; 0.03 S	[27]
Y05	2205	Bal	21.1	5.8	2.7	0.02	1.42	0.45	0.052	0.165	0.025 P; 0.022 S	[8]
S07	2507	Bal	25.22	6.94	3.9	nr	0.46	0.25	0.011	0.287	0.019 P; 0.0006 S	[6]

nr = not reported

Table 1.1.3. Austenite content and tensile properties of duplex stainless steels (prior to hydrogen exposure) used to study hydrogen effects.

Material	Austenite content (%)	Strain rate (s^{-1})	S_y (MPa)	S_u (MPa)	El_t (%)	RA (%)	Ref.
Z91A - L	37	10^{-4}	651	795	42	84	[4]
Z91A - T			634	785	41	74	
Z91B - L	35		620	740	36	85	
Z91B - T			600	710	39	83	
Z91B	35	—	577	766	36	87	[3]
E96	35	—	623	744	42	78	[5]
E96 - 50	50	3.7×10^{-6}	592	758	39.1	80.5	[2]
E96 - 15	15		704	807	30.6	64.7	
E96 - 0	0		743	844	19.9	51.7	

L = Longitudinal, T = Transverse

Table 3.1.1.1. Smooth tensile properties of duplex stainless steel at room temperature; measured in air with internal hydrogen (thermal precharging in hydrogen gas).

Material	Thermal precharging	Test environment	Strain rate (s^{-1})	S_y (MPa)	S_u (MPa)	El_u (%)	El_t (%)	RA (%)	Ref.
2507, heat S07 annealed	None	Air	1.2×10^{-3}	647	879	25	48	85	[6]
	(1)	Air		745	914	24	35	46	
2507, heat S07 strain-hardened	None	Air	1.2×10^{-3}	988	1110	1.2	26	80	[6]
	(1)	Air		1208	1221	1.0	12	25	

(1) 138 MPa hydrogen, 573 K, 240 h (saturation); measured average concentration of 125 wppm hydrogen (7000 appm)

Table 3.2.1.1. Fracture toughness of duplex stainless steel at room temperature; measured in air with internal hydrogen (thermal precharging in hydrogen gas).

Material	Test method	Thermal precharging	Test environment	S_y † (MPa)	K_{IC} (MPa $m^{1/2}$)	Ref.
2507, heat S07 strain-hardened	3PB LEFM & EPFM	None	Air	988	285 ‡	[6]
		(1)	Air	1208	48	

3PB = 3-point bending specimen, LEFM = linear elastic fracture mechanics, EPFM = elastic-plastic fracture mechanics

† yield strength of smooth tensile specimen

‡ value determined from J_Q (i.e. specimen did not meet the geometrical requirements of ASTM E1820 for K_{IC} or J_{IC})

(1) 138 MPa hydrogen, 573 K, 1440 h (saturation); measured average concentration of 125 wppm hydrogen (7000 appm)

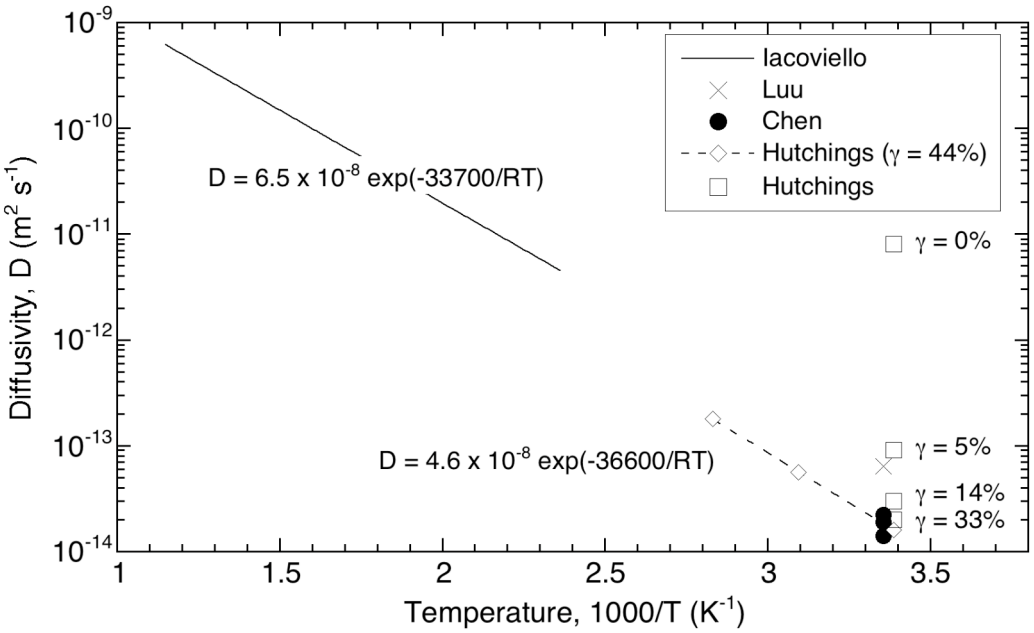

Figure 2.1. Hydrogen diffusivity as a function of temperature for several duplex alloys: Iacoviello, heat I97 [14]; Luu, heat L02 [27]; Chen, heat L02, values for annealed, cold-worked 20% and 40% respectively in increasing order of diffusivity [16]; Hutchings, heat H91 [12, 13].

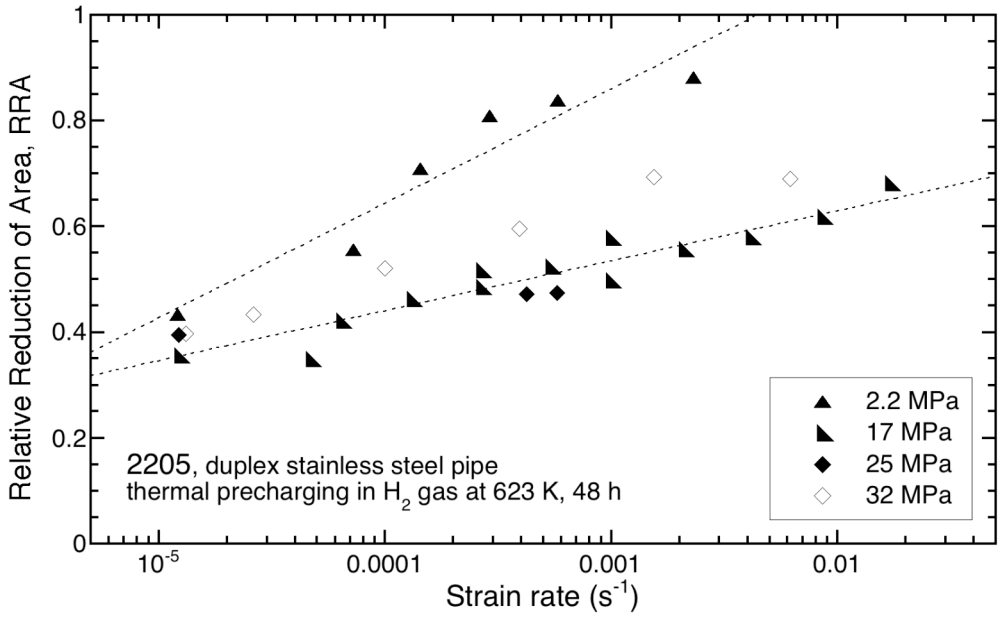

Figure 3.1.1.1. Relative reduction of area of 2205 duplex stainless steel as a function of strain rate in smooth tensile tests. The material has been thermally precharged with hydrogen at 623 K and several hydrogen gas pressures: closed symbols heat Z91B from Ref. [3]; open symbols heat E96 from Ref. [5].

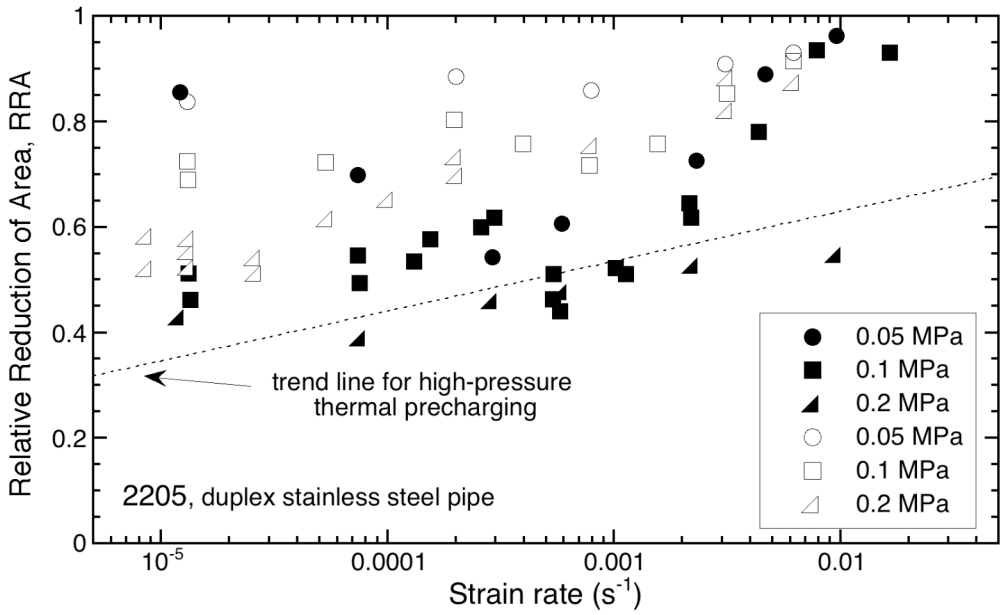

Figure 3.1.1.2. Relative reduction of area for 2205 duplex stainless steel as a function of strain rate in smooth tensile tests. Tests were conducted in hydrogen gas at room temperature and several hydrogen gas pressures: closed symbols heat Z91B from Ref. [3]; open symbols heat E96 from Ref. [5]. Trend line from Figure 3.1.1.1.

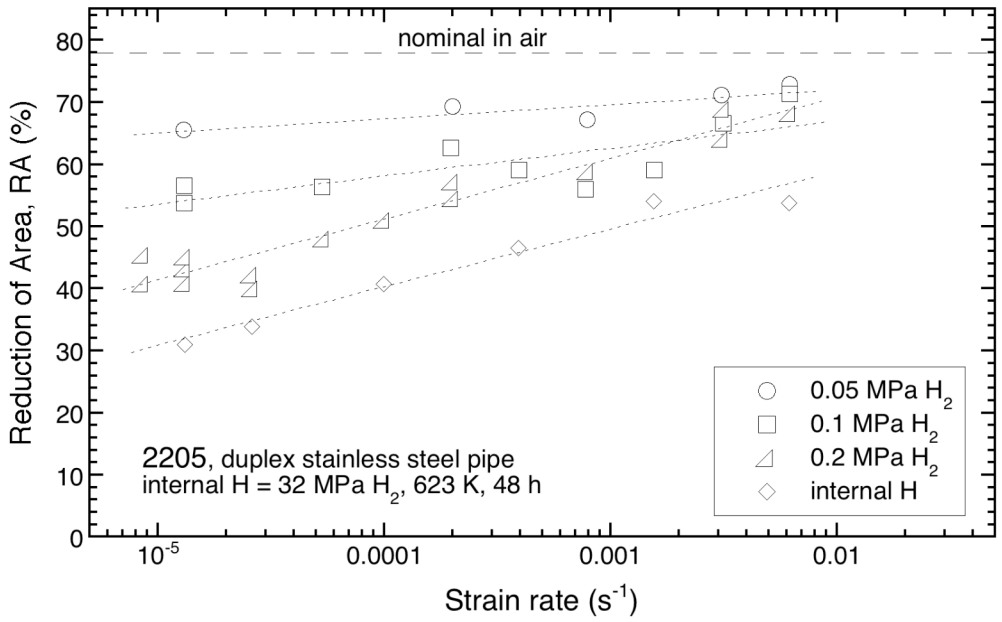

Figure 3.1.1.3. Reduction of area for 2205 duplex stainless steel (heat E96) as a function of strain rate in smooth tensile tests comparing internal and external hydrogen. Same data as from Figure 3.1.1.1 and 3.1.1.2. [5]

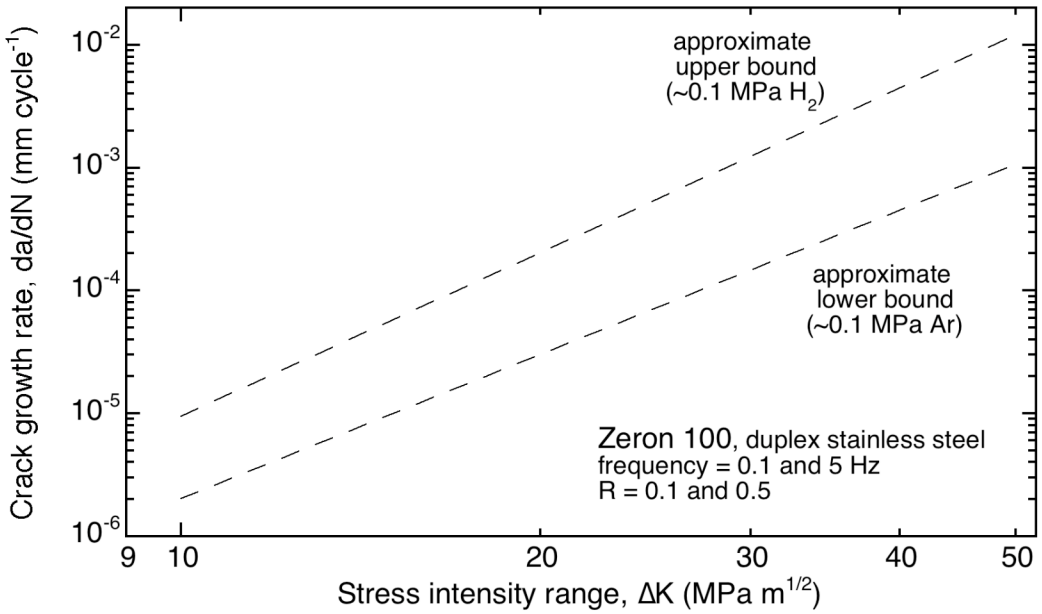

Figure 3.3.1. Approximate bounds for crack growth of compact tension specimens (heat M91) in approximately 0.1 MPa gas, R = 0.5. Crack growth rates are independent of frequency at 0.1 and 5 Hz. The crack growth rate is intermediate between these bounds for R = 0.1 in hydrogen at low ΔK, but converges to the upper bound at high ΔK. [10]

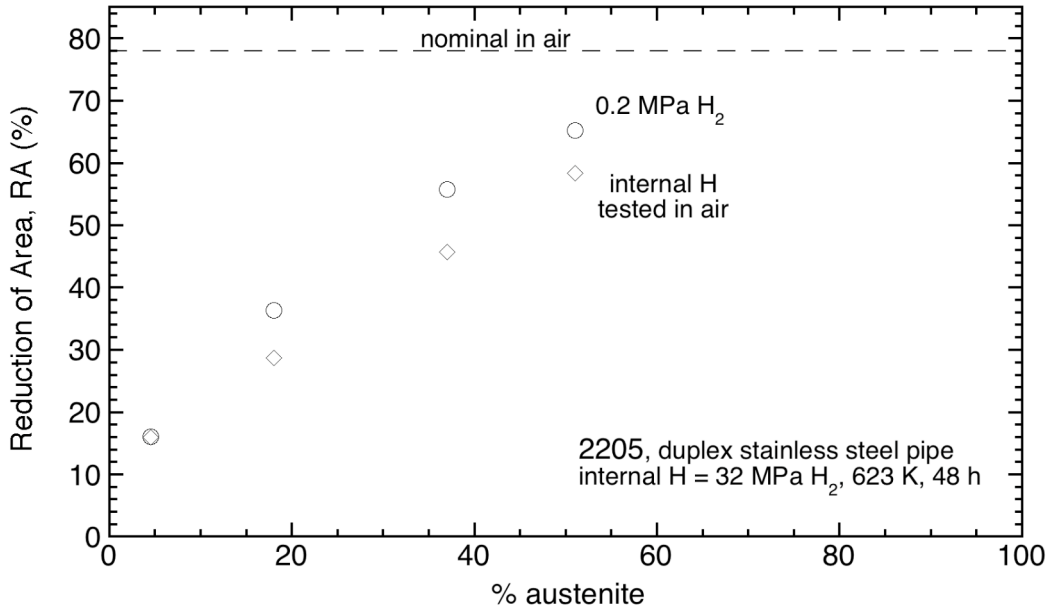

Figure 4.1.1. Reduction of area for 2205 duplex stainless steel (heat E96) as a function of austenite content with internal hydrogen and in external hydrogen. [2]